

# Development of a rational design methodology for precast concrete slender spandrel beams: Part 1, experimental results

**Gregory Lucier, Catrina Walter, Sami Rizkalla, Paul Zia, and Gary Klein**

## Editor's quick points

- This article is the first part of a two-part paper that studies detailing requirements for the end regions of precast concrete slender spandrel beams.
- An extensive experimental program was undertaken to develop a rational design procedure for precast concrete slender spandrel beams.
- The experimental results, combined with the analytical results and rational modeling in the companion paper, demonstrate that properly designed open web reinforcement is a safe, effective, and efficient alternative to traditional closed stirrups for precast concrete slender spandrel beams that have an aspect ratio of 4.6 or greater.

Precast concrete slender spandrel beams are commonly used in parking structures to transfer vertical loads from deck sections to columns. In addition, slender spandrels often serve as a railing or barrier around the exterior edge of the parking structure. Large single-tees or double-tees frequently serve as deck sections and generally span 40 ft to 65 ft (12 m to 20 m).

Typical slender spandrel beams are from 5 ft to 7 ft (1.5 m and 2.1 m) deep with spans ranging from 30 ft to 50 ft (9.1 m to 15 m). These beams usually have a web thickness of at least 8 in. (200 mm). Spandrels that have a large aspect ratio (defined as the spandrel height divided by the thickness of the web) are commonly considered slender members. In this investigation, spandrels with aspect ratios of 4.6 and 7.5 were tested.

In many cases, a continuous ledge runs along the bottom edge of the web on one side of the beam, resulting in what is known as an L-shaped spandrel. The ledge is used to provide bearing for the deck sections, so the L-shaped slen-

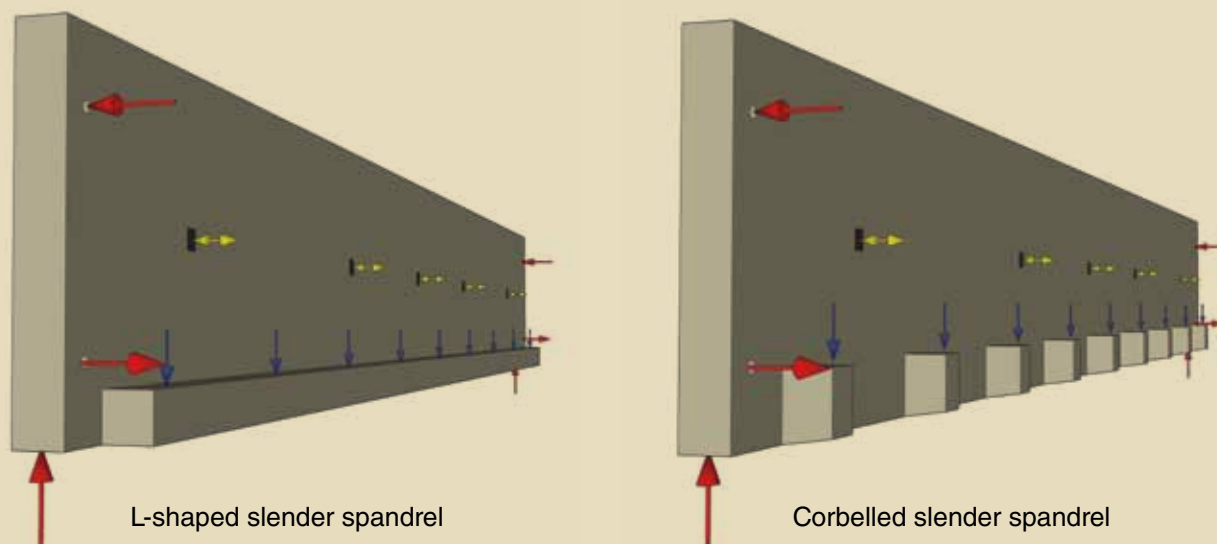


**Figure 1.** Typical L-shaped and corbelled slender spandrels. Note: Blue arrows show applied loads, red arrows show supporting reactions, and yellow arrows show forces at the deck connections.

der spandrel beam is subjected to a series of discrete eccentric loadings (**Fig. 1**). A common alternative configuration is a corbelled slender spandrel beam, where the continuous ledge is replaced by a series of discrete haunches (**Fig. 1**). In both configurations, the web of the slender spandrel is supported vertically on a simple span and is secured laterally to a column at each end through two discrete web tiebacks. In addition, the precast concrete deck sections are generally attached to the inner web face of the slender spandrel through welded connections along the length. The eccentric vertical loading and unsymmetrical cross section result in flexure, shear, and torsional stresses acting on the beam. Slender spandrel behavior is heavily influenced by shear- and torsional stresses in the end region, which act in the same direction on the inner web face and oppose one another on the outer web face. The effects of shear and torsion are greatest in the end regions, as dictated by the vertical and lateral supports.

There exists a substantial body of literature relevant to the design of reinforced and prestressed concrete members for torsion and for the interaction of torsion, shear, and flexure.<sup>1-4</sup> A review of literature relevant to the torsion design of structural concrete can be found in section 7 of Technical Report IS 09-10,<sup>5</sup> which presents all details, results, and findings of the research.

The approach to shear and torsion design recommended by the American Concrete Institute's (ACI's) *Building Requirements for Structural Concrete (ACI 318-08)* and *Commentary (ACI 318R-08)*<sup>6</sup> assumes that the member response just before failure will be characterized by spalling of the concrete shell outside of the stirrups, leaving a core of confined concrete to resist shear and torsion. Researchers have recommended closed stirrups with 135 deg hooks

to maintain the integrity of the core after spalling. These detailing requirements often result in tightly congested, interwoven reinforcement, especially in the end regions.

The precast concrete industry currently designs slender spandrel beams subjected to combined loading using an approach developed by Zia and Hsu,<sup>4</sup> which is outlined in the sixth edition of the *PCI Design Handbook: Precast and Prestressed Concrete*.<sup>7</sup> The *PCI Design Handbook* method is based on assumptions similar to those made by the ACI 318-08<sup>6</sup> approach, including behavior marked by spiral cracking in the concrete and face shell spalling. Section 11.5.7 of ACI 318-08 references the Zia-Hsu procedure as a permissible alternative method for torsion design of cross sections having an aspect ratio of 3 or greater. The design method can be used for prestressed or conventionally reinforced concrete beams and is commonly used to proportion shear and torsion reinforcement in the webs of slender spandrel beams. Zia and Hsu developed their design method based on tests of the sectional torsional strength of compact rectangular specimens that have aspect ratios of 3 or less, and the procedure was never intended to be used for slender cross sections. Although the Zia-Hsu approach has proved safe and reliable for slender spandrels, it typically requires large quantities of severely congested vertical and longitudinal reinforcement, particularly in the end regions of slender beams.

## Objective

The main objective of this research program was to develop rational design guidelines for precast concrete slender spandrel beams. These design guidelines, presented in a companion paper,<sup>8</sup> are expected to simplify the reinforcement detailing required for slender spandrels, especially in

**Table 1.** Test matrix

Depth, in.	Span, ft	Aspect ratio, $h/b$	Designation	Configuration		
				L-shaped	Corbel	
60	30	7.5	SP1.8L60.30.P.O.E*	X		
			SP2.8L60.30.P.O.E*	X		
60	45		SP3.8L60.45.P.O.E*	X		
			SP4.8L60.45.P.O.E*	X		
60	45	7.5	SP10.8L60.45.R.O.E	X		
			SP11.8L60.45.R.C.E	X		
			SP12.8L60.45.P.O.E	X		
			SP13.8L60.45.P.C.E	X		
			SP14.8L60.45.P.O.T	X		
			SP15.8L60.45.P.O.T	X		
			SP16.8L60.45.R.O.T	X		
			SP17.8CB60.45.P.O.E		X	
			SP18.8CB60.45.P.S.E		X	
			SP19.8CB60.45.P.O.T		X	
46	45	4.6	SP20.10L46.45.P.O.E	X		
			SP21.10L46.45.P.O.T	X		

\*Specimens were sponsored privately by individual PCI Producer Members.

†SP18 was constructed with special closed reinforcement in a hooked-C shape.

Note:  $b$  = web thickness;  $h$  = beam height. 1 in. = 25.4 mm; 1 ft = 0.305 m.

the end regions. Specifically, the research focused on investigating whether traditional closed stirrups were required for the slender cross sections of typical precast concrete L-shaped and corbelled spandrels. The use of open reinforcement in lieu of closed stirrups would greatly simplify fabrication and reduce the cost of production.

## Experimental program

The experimental program was part of a larger research effort, which also included analytical studies based on three-dimensional nonlinear finite-element models, rational analyses, and the development of a simple rational design procedure.

In total, 16 precast concrete spandrel beams were tested to failure. All specimens were full-scale beams, most spanning 45 ft (13.7 m). Two beams were tested at a 30 ft (9.1 m) span. Each specimen was loaded through associated full-scale double-tee deck sections to mimic typical field conditions. Prior to final failure testing, all spandrels were loaded to several stages of interest, including the full service load and the factored design load, and measurements

and observations were made at each stage. In the case of the factored design load, the load was held on each beam for 24 hours to evaluate the performance under sustained load.

Two test specimens were designed and detailed with closed stirrups, according to current practice, to serve as controls. The remaining specimens were designed with various configurations of open web reinforcement. The open transverse web reinforcement was proportioned in the test specimens using ACI 318-08<sup>6</sup> procedures without considering torsion. Additional transverse reinforcement was provided on the inner web face based on plate bending about a 45 deg inclined crack. In both cases, ACI 318-08 strength reduction factors were considered. These procedures are explained in detail in the companion paper.<sup>8</sup>

**Table 1** shows other parameters included in the test matrix. All specimens were supported using Teflon-coated bearing pads unless otherwise noted in the table. The parameters in the test matrix are described in the next section along with the labeling convention used to identify each specimen.

	Concrete		Reinforcement		Detailing		Bearing	
	Prestressed	Reinforced	Open	Closed	Enhanced	Typical	Teflon	Typical
	X		X		X		X	
	X		X		X			X
	X		X		X		X	
	X		X		X		X	
		X	X		X		X	
		X		X	X		X	
	X		X		X		X	
	X			X	X		X	
	X		X			X	X	
	X		X			X		X
		X	X			X	X	
	X		X		X		X	
	X			X <sup>†</sup>	X		X	
	X		X			X	X	
	X		X		X		X	
	X		X			X	X	

## Parameters

**Open versus closed reinforcement** The primary variable considered in this experimental program was the use of open web reinforcement. Thirteen of the sixteen experimental specimens were designed and fabricated with open web reinforcement. The two control specimens were reinforced with traditional closed stirrups. Another specimen, SP18, was fabricated with partially closed reinforcement including inner-face vertical steel hooked over the top and bottom of the beam. This specimen was not intended to be a practical design option but was included to serve as a direct comparison between a companion beam reinforced with an identical amount of web steel without the hooks. **Figure 2** shows sketches of a typical L-shaped spandrel cross section with typical open and closed web reinforcement schemes. In addition, the same figure shows a sketch of the special partially closed reinforcement scheme used for SP18.

In this research program, open reinforcement included flat sheets of welded-wire reinforcement (WWR); conventional deformed reinforcing bars bent into L, C, or U shapes; and straight bars or tendons. An open web reinforcement

scheme used in several specimens was the combination of WWR on the outer spandrel face and L-shaped bars on the inner spandrel face. As discussed, the primary advantage of using open reinforcement compared with traditional closed stirrups is the ease of fabrication.

**Production of open versus closed reinforcement** A significant advantage in using open web reinforcement was the efficiency gained in production. Observations made during the production of the experimental beams indicate that assembling an open reinforcing cage took 30% to 50% less time than assembling a traditional closed reinforcing cage. The gains in efficiency were especially obvious when an open cage was produced on the same form line adjacent to a closed cage, as was the case for SP12 and SP13. In producing the open cage (with the spandrel lying outer-face down on the form), the outer-face web reinforcement (often WWR) was placed in the empty form first. The strands were then pulled and stressed without obstructions. After stressing the strands, any required longitudinal steel bars, such as U-bars in the end regions, were simply placed in the form near their final locations.

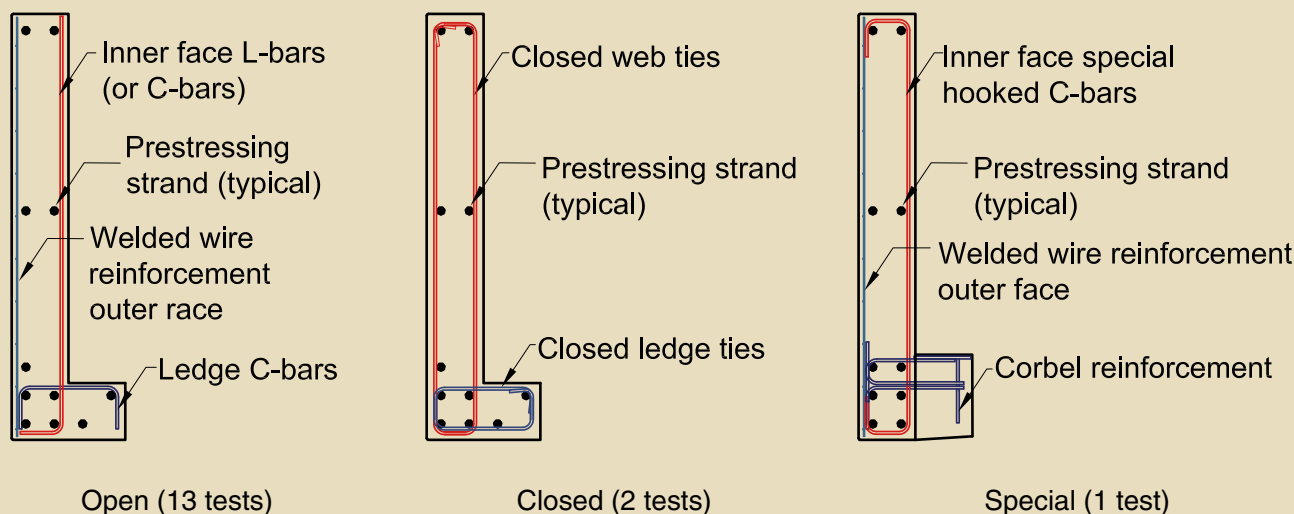


**Figure 2.** Open and closed reinforcement schemes used on typical L-shaped slender spandrel cross section and special web reinforcement scheme on a typical corbelled slender spandrel.

With the strands stressed, the other components of the open reinforcing cage were dropped into the form at the correct locations and tied into place. L-shaped or C-shaped bars on the inner spandrel face were placed so that they rested on the stressed strands. C-shaped ledge bars or corbel assemblies were hooked around the longitudinal steel and secured to strands or bars. With the web steel in place, the additional longitudinal U-bars were secured. The flexibility of the open reinforcement allowed for spacing of the bars to be easily adjusted as the cage was finalized. If a bar was misplaced, it could be removed and replaced without disrupting any other components of the cage.

The stirrups (both web and ledge) had to be placed in the empty form for the closed reinforcing cages. During this step, it was important to verify that the sequence of the stirrups corresponded to their final locations in the beam. With the stirrups in the form, the prestressing strands, along with any other required longitudinal steel, were threaded through the stirrups, taking care not to disrupt the stirrup order. The strands were then prestressed.

After stressing the strands, the stirrups and additional longitudinal bars were spaced and secured in place at their final locations. If errors were made in placing the stirrups in a closed cage, few options were available to correct them, short of detensioning the strands. Misplaced stirrups could be cut and removed from the cage, but inserting replacement or additional stirrups was a challenge. In some cases, the side rails of the form could be removed and any missing stirrups bent into place around the already-stressed strands, but this procedure required significant effort. Careful planning and layout at the start of a closed-cage assembly can minimize mistakes, but even infrequent assembly errors can be costly with a closed reinforcement cage.

In addition to gains in production efficiency, the use of

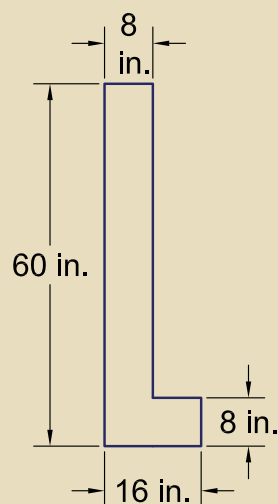
an open reinforcement cage offered significant savings in steel compared with traditional designs using closed stirrups. In examining the test specimens in this program, an open reinforcement cage required up to 50% less shear and torsion steel than a comparable closed cage.

The difference in required steel can be highlighted for SP10 and SP11. Both specimens were slender spandrels with 60 in.  $\times$  8 in. (1500 mm  $\times$  200 mm) webs and 45 ft (13.7 m) spans. Both contained extra reinforcement for flexure to ensure end-region failures. SP10 was designed with open web reinforcement, while SP11 was designed with traditional closed stirrups. Both were designed for the same applied loads. Flexural reinforcement was the same for both specimens and is excluded from the calculated steel quantities. The total quantity of steel used to produce SP10 was 715 lb (3180 N), compared with 1396 lb (6209 N) required to produce SP11 (both weights exclude the common flexural steel). The 681 lb (3030 N) difference is equivalent to a 48% reduction in web steel.

A similar analysis was performed on prestressed beams SP12 and SP13. Neglecting the flexural steel common to both beams, the steel required for the open cage of SP12 was 778 lb (3460 N) compared with 1251 lb (5564 N) for the closed cage of SP13. The 473 lb (2100 N) difference is equivalent to a 37% reduction in web steel. Additional details of the reinforcement for these beams are reported elsewhere.<sup>5</sup>

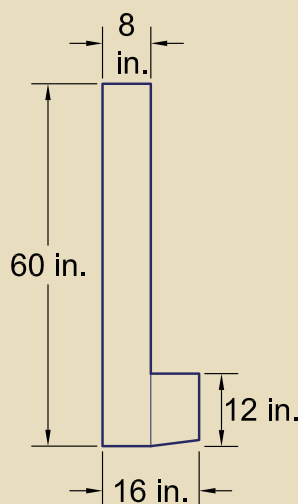
**Continuous ledge versus corbels** The two types of precast concrete slender spandrel beams considered in this experimental program were L-shaped and corbelled spandrels. Both types are commonly used. Figure 1 shows the two types of spandrels.

**Span** Specimens with two span lengths, 30 ft (9.1 m) and 45 ft (13.7 m), were tested.



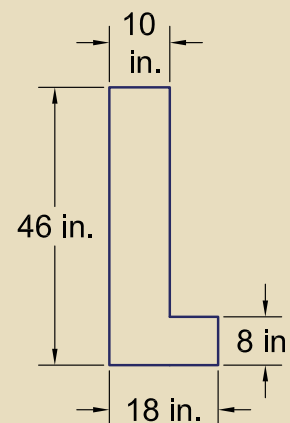
L-shaped spandrel  
Aspect ratio = 7.5

11 Beams  
30 ft and 45 ft spans



Corbelled spandrel  
Aspect ratio = 7.5

3 Beams  
45 ft span



L-shaped spandrel  
Aspect ratio = 4.6

2 Beams  
45 ft span

**Figure 3.** Cross sections of tested spandrels. Note: 1 in. = 25.4 mm; 1 ft = 0.305 m.

**Aspect ratio** Aspect ratio is defined as beam height divided by web thickness ( $h/b$ ). The two aspect ratios studied in this experimental program were 4.6 and 7.5. Fourteen L-shaped and corbelled spandrels were tested with 8-in.-thick  $\times$  60-in.-deep (200 mm  $\times$  1500 mm) webs, giving an aspect ratio of 7.5. The lateral tiebacks at the support for these beams were spaced 36 in. (910 mm) apart, centered in the height of the web. In addition, two L-shaped spandrels were tested with a web thickness of 10 in. (250 mm) and a web depth of 46 in. (1200 mm) for an aspect ratio of 4.6. The lateral tiebacks at the support for these beams were spaced 32 in. (810 mm) apart and centered in the height of the web. **Figure 3** shows the three spandrel cross sections considered in the experimental program.

#### Prestressed versus reinforced concrete

Thirteen of the sixteen specimens were designed with prestressed tendons as the primary flexural reinforcement. The remaining three specimens were reinforced with conventional mild-steel deformed bars as the only flexural reinforcement.

#### Typical versus enhanced reinforcement

A slender precast concrete spandrel beam would typically fail in flexure if it were loaded beyond the factored design load. For the purposes of investigating end-region behavior, however, it was necessary to force failures to take place in the end regions. Therefore, a number of selected beams were designed to fail in their end regions by using extra reinforcement for flexure. In addition, the ledges or corbels

of these selected beams were also strengthened to prevent punching shear or other localized failure modes.

In strengthening the selected test specimens against possible failure modes outside their end regions, care was taken to avoid enhancing the end-region shear and torsion strength. The reserve flexural strength was provided by adding mild steel bars at the midspan of specimens otherwise designed with normal levels of flexural reinforcement. When provided, the additional bars were terminated well outside the end regions. In addition, steel angle details were provided in the ledges of selected L-shaped spandrel specimens in the localized area underneath each double-tee stem. These welded details enhanced the ability of the ledge to resist punching shear without altering the shear and torsion strength of the cross section.

Extra hanger reinforcement was provided in the middle region of some beams to prevent separation of the ledge or corbel from the web. While 11 of the 16 test beams were designed to induce end-region failures, the remaining 5 specimens were designed with typical amounts of flexural, ledge or corbel, and hanger reinforcement at all locations, as recommended by the *PCI Design Handbook*.<sup>7</sup> These specimens were included in the test matrix to examine the behavior and to determine the failure modes of specimens reinforced with open web reinforcement but otherwise detailed according to current practice.

Beams designated in the test matrix as having enhanced



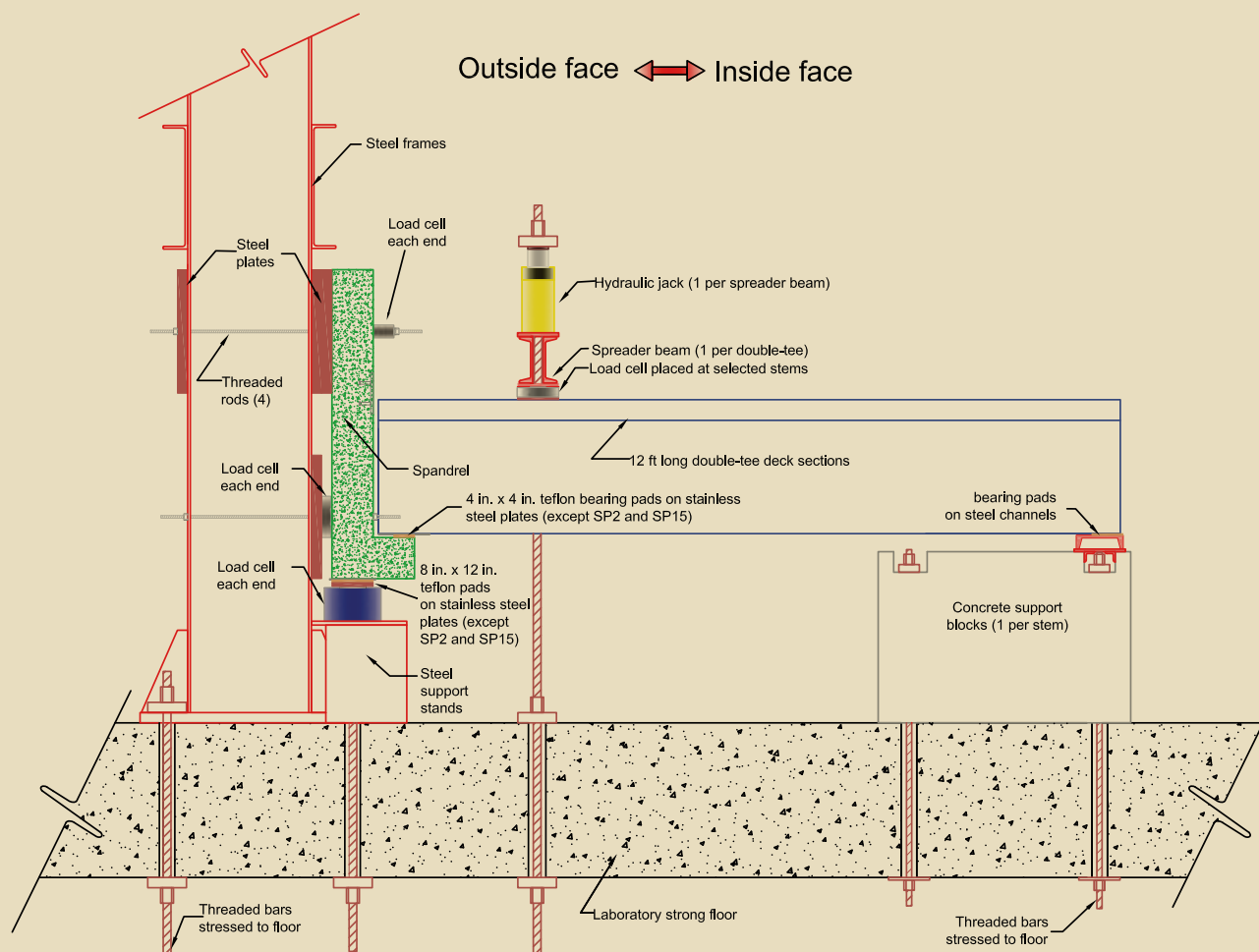


**Figure 4.** Profile of the test setup. Note: 1 in. = 25.4 mm; 1 ft = 0.305 m.

detailing included the additional reinforcement described. Beams designated as having typical detailing were designed according to *PCI Design Handbook* recommendations.<sup>7</sup> The typical specimens are representative of beams that would be designed for an actual project, while the enhanced specimens were included to allow detailed study of end-region behavior and failure modes.

**Bearing pads** Two different types of bearing pads were used in the experimental tests: common randomly oriented fiber and rubber composition pads and Teflon-coated preformed fabric pads. Bearing pads were located between each double-tee stem and the ledge or corbel. Bearing pads were also located between the spandrel and the support at each end of the beam. Although randomly oriented fiber and rubber composition pads are commonly used by the industry in parking garages, these pads have a relatively low stiffness and a relatively high coefficient of friction. Bearing-pad friction helps to decrease the out-of-plane movement of a slender spandrel by providing a horizontal stabilizing reaction at every double-tee stem; however, the benefit of this bearing friction should not be relied on in design. Thus, Teflon-coated, preformed fabric bearing

pads and polished stainless steel plates were used in the majority of the tests to eliminate bearing-pad friction as much as possible, thereby creating a test condition more severe than is likely to occur in the field. Conventional randomly oriented fiber and rubber composition bearing pads were used only for two of the sixteen tests to investigate the effect of bearing pad friction on slender spandrel behavior.

## General test setup

The framework used to test all spandrels was designed around a strong floor in the testing laboratory. The test setup consisted of the following primary components:

- a system of columns, beams, and stands designed to transfer the vertical and horizontal reactions of the spandrels to the strong floor with minimal support deflections
- a system of spreader beams, tie-down rods, and hydraulic jacks designed to produce the required load and transfer it evenly to the appropriate points on the

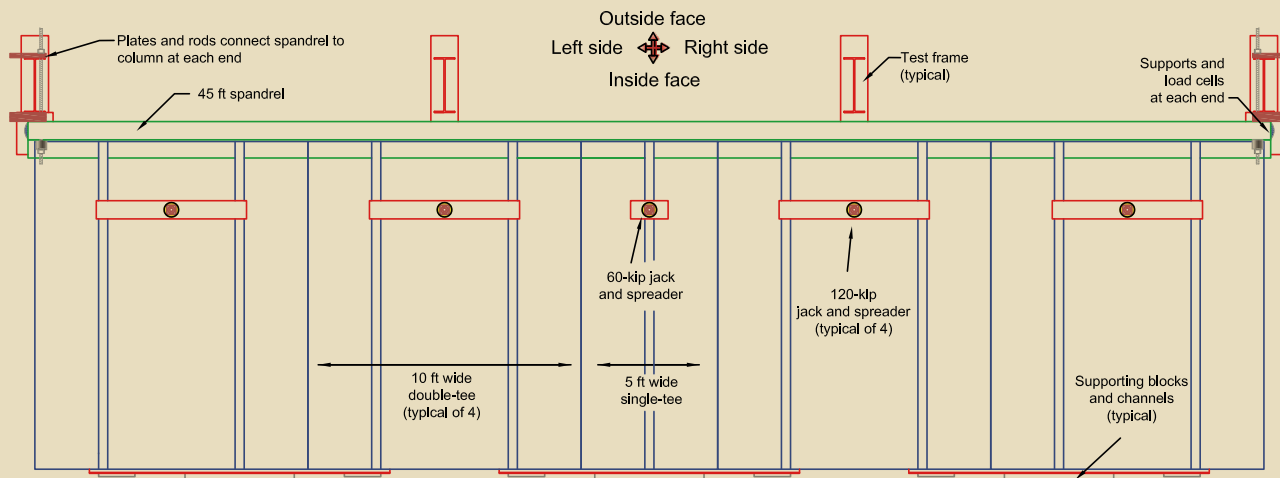


**Figure 5.** Top view of a typical 45 ft (13.7 m) test setup. Note: 1 ft = 0.305 m; 1 kip = 4.448 kN.

#### test specimens

- a system of concrete support blocks, steel channels, and tie-down rods to support the end of the double-tee deck opposite the spandrel
- an array of load cells and other instrumentation used to measure data loads, deformations, and strains

**Figure 4** shows a sketch of the test configuration; **Fig. 5** shows a plan view of the test setup for the 45 ft (13.7 m) spandrels. Labeling conventions for inside, outside, left, and right are also established in these figures and will be used throughout this paper. Further information on the test setup is reported elsewhere.<sup>1</sup>

**Instrumentation** About 40 instruments recorded data during each test. Four basic types of instrumentation were used. All instruments were connected to an electronic data acquisition system. Additional details of the instrumentation used are reported elsewhere.<sup>5</sup>

- Load cells were used to measure the vertical and lateral spandrel reactions and to measure the load applied by the jacks. In addition, a pressure transducer was used to record the pressure applied by the hydraulic pump.
- String and linear potentiometers (pots) were used to measure vertical and lateral displacements of the spandrel.
- Inclinometers were used to measure the rotation of each spandrel at the quarter points.
- Pi gauges were used to measure concrete strains on the top, bottom, and inside face of each spandrel.

#### Loading

All loads other than the spandrel self-weight were transferred to the spandrel through the stem reactions of 10DT26 deck sections. The stems were spaced evenly along the ledge or corbels of each spandrel at 5 ft (1.5 m) on center. The double-tee bearing pads were centered 2 in. (50 mm) back from the edge of the ledge and 6 in. (150 mm) from the inner face of the web.

Designs of the tested specimens were based on a live load LL of 40 lb/ft<sup>2</sup> (1.92 kN/m<sup>2</sup>) and a snow load SL of 30 lb/ft<sup>2</sup> (1.44 kN/m<sup>2</sup>). The dead load DL included the self-weight of the spandrel beam and the 71.6 lb/ft<sup>2</sup> (3.43 kN/m<sup>2</sup>) weight of the double-tee decks. The controlling factored load case of 1.2DL + 1.6LL + 0.5SL was considered. The vertical end reaction of each simply supported spandrel was monitored throughout testing and served as the basis for controlling a loading system of hydraulic jacks during the test. Thus, all discussion of load levels refers to the main vertical reaction for a given beam.

Load combinations other than the factored load were also important for the tests. Load levels considered during testing included service load without snow (DL + LL), the reduced service load with snow specified by the American Society of Civil Engineers' (ASCE's) *Minimum Design Loads for Buildings and Other Structures* (7-10)<sup>9</sup> (DL + 0.75LL + 0.75SL), service load with full snow load (1.0DL + 1.0LL + 1.0SL), and the ACI 318-08<sup>6</sup>/ASCE 7-10 factored design load (1.2DL + 1.6LL + 0.5SL). Three types of spandrels were tested with a 45 ft (13.7 m) nominal span. These three types include the 8 in. × 60 in. (200 mm × 1500 mm) L-shaped spandrel, 8 in. × 60 in. corbelled spandrel, and 10 in. × 60 in. (250 mm × 1500 mm) L-shaped spandrel. To simplify testing and comparison, the design loads for all spandrel types were considered to be the same because the differences in self-weight among the



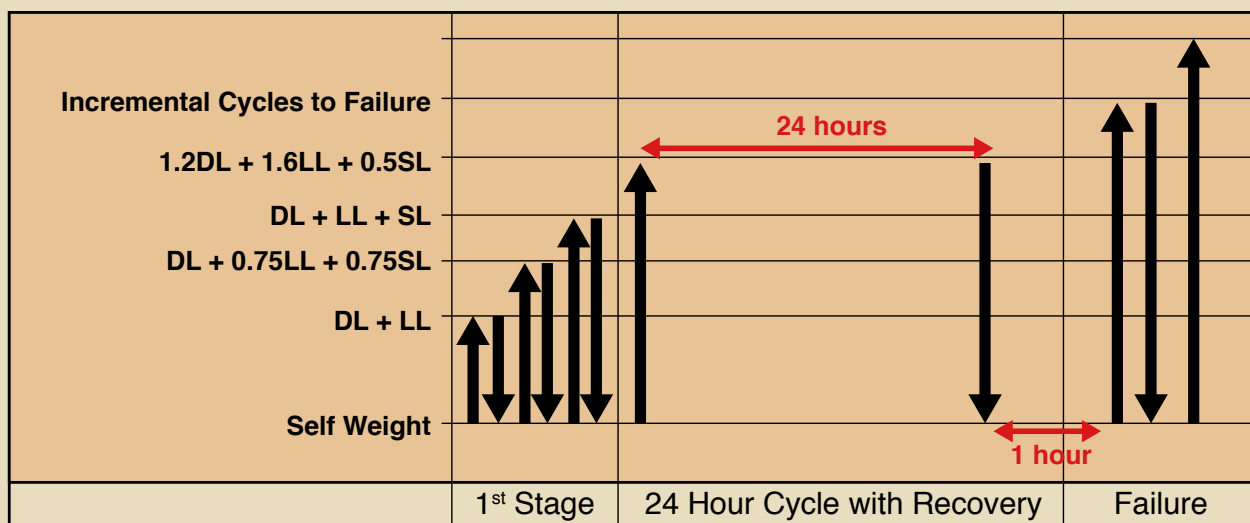


**Figure 6.** Typical loading sequence. Note: DL = dead load, LL = live load, SL = snow load.

three selected cross sections were negligible.

References to dead load assume that the experimental spandrels are supporting the reaction of a 60-ft-span (18 m) double-tee deck. Due to space limitations, however, a 12-ft-span (3.7 m) double-tee deck was used in the tests. Thus, the dead-load condition was equivalent to the self-weight of the test spandrel. The portion of the stem reactions resulted from the self-weight of the 12 ft deck sections, and the remainder of the stem reactions were generated by the jacking system to represent the full reaction of a 60-ft-span double-tee deck.

**Figure 6** shows the loading sequence for a typical test. Each spandrel was loaded to the first selected level (service load) and held at this level to allow for observations and marking of cracks. The loading was also paused on the way to the service load to check for initial cracking. After making observations at the service load, each spandrel was unloaded and then reloaded to the next selected level and additional observations were made. This process was repeated until the factored load level was reached. Initial observations were made at the factored load level, and this load was held on each beam for 24 hours, exceeding the requirements of sustained load tests for in-place structures as outlined in chapter 20 of ACI 318-08.<sup>6</sup> After 24 hours, the spandrel was unloaded from the factored load, and its recovery was monitored for 1 hr to check the recovery criterion specified in ACI 318-08. Finally, each spandrel was loaded and unloaded incrementally beyond the factored load until failure occurred.

## Results

Data and detailed observations for all 16 beams in the experimental program are documented elsewhere.<sup>5</sup> **Table 2** gives a summary of results for all tested specimens.

### Cracking pattern on the inner web face

The observed cracking patterns had similar characteristics for all spandrels, regardless of configuration, reinforcement, or aspect ratio. The inner-face cracking pattern was the tied-arch type, previously documented by other researchers.<sup>10-13</sup> The observed behavior of the slender spandrel beams also indicates that the effects of shear and torsion dominate in the disturbed end region. This end region is followed by a transition region where the effects of shear and torsion gradually decrease along with increasing effects of flexure. Beyond the transition region, flexural effects dominate slender spandrel behavior.

During each test, cracks were marked on the surface of each spandrel at several load levels of interest. Spandrels were whitewashed prior to testing to make cracks more visible. In all tests, inner-face cracking initiated near the support and extended upward toward midspan from each end of the beam at an angle of about 45 deg. These cracks gradually flattened out and arched toward the center of the beam. Vertical cracks initiating from the bottom of the beam were observed on the inner web face near midspan for all tests. Localized cracking was observed around the concentrated loads in the ledge or corbels. **Figure 7** shows the inner-face cracking pattern typical of all tests for a representative continuous L-shaped spandrel beam, and **Fig. 8** shows that of a corbelled spandrel.

### Cracking pattern on the outer web face

The observed outer-face cracking patterns were also similar for all tested beams. **Figure 9** shows the observed outer-face cracking pattern for a typical beam with an aspect ratio of 7.5. As with the inner-face cracking patterns,

**Table 2.** Summary of failure load and failure mode for all tested beams

Spandrel	Spandrel reaction		Lateral reactions at failure, kip				Description of failure mode
	Failure, kip	Factored, kip	Top left	Top right	Bottom left	Bottom right	
SP1.8L60.30.P.O.E	135	84.8	23.3	21.3	29.9	25.2	Failure of the spandrel ledge to web attachment
SP2.8L60.30.P.O.E common randomly oriented fiber and rubber composition pads	150	84.8	14.2	16.3	16.5	17.0	Shear failure in the stem of one double-tee used for loading
SP3.8L60.45.P.O.E	196	126.6	32.4	34.4	38.9	42.9	Spandrel failure along a skewed-diagonal crack in the right end region
SP4.8L60.45.P.O.E	200	126.6	34.5	29.3	38.0	40.0	Spandrel failure along a skewed-diagonal crack in the left end region.
SP10.8L60.45.R.O.E	208	126.6	27.7	28.3	50.2	46.0	Spandrel failure along a skewed-diagonal crack in the left end region.
SP11.8L60.45.R.C.E	251	126.6	35.8	33.1	47.9	45.8	Test terminated due to impending ledge punching, localized concrete crushing at top of section, and heavy cracking through the web between the lateral connections
SP12.8L60.45.P.O.E	185	126.6	23.7	28.0	35.3	42.6	Spandrel failure along a skewed-diagonal crack in the left end region
SP13.8L60.45.P.C.E	240	126.6	41.0	37.8	57.4	54.3	In-plane flexural failure near midspan
SP14.8L60.45.P.O.T	160	126.6	22.6	22.6	25.4	27.9	Punching shear failure of the ledge at midspan underneath the single-tee stem
SP15.8L60.45.P.O.T common randomly oriented fiber and rubber composition pads	140	126.6	19.2	19.6	20.6	21.4	Punching shear failure of the ledge 10 ft from midspan, underneath the third double-tee stem from the right end
SP16.8L60.45.R.O.T	127	126.6	16.9	16.9	19.0	19.0	Punching shear failure of the ledge beneath the first double-tee stem on the left end of the spandrel (failure occurred prior to completion of 24-hour load test)
SP17.8CB60.45.P.O.E	200	126.6	30.3	20.2	36.3	36.3	Spandrel failure along a skewed-diagonal crack in the right end region
SP18.8CB60.45.P.S.E	220	126.6	27.3	25.3	45.1	45.1	Spandrel failure along a skewed-diagonal crack in the right end region
SP19.8CB60.45.P.O.T	173	126.6	18.5	18.8	26.4	30.9	Corbel failure at midspan
SP20.10L46.45.P.O.E	171	126.6	27.4	26.6	30.8	28.6	Spandrel failure along a skewed-diagonal crack in the right end region
SP21.10L46.45.P.O.T	127	126.6	24.4	29.4	25.0	24.3	In-plane flexural failure near midspan (failure occurred prior to completion of 24-hour load test)

Note: 1 ft = 0.305 m; 1 kip = 4.448 kN.



**Figure 7.** Inner-face cracking pattern for a representative L-shaped spandrel (digitally enhanced cracks).

the outer-face patterns were symmetrical about midspan. Initial cracks on the outer face were usually observed near midspan, where a region with only vertical cracks initiated from the bottom of the beam. Near the ends of a beam, cracks were observed extending downward from the top lateral reaction. These cracks developed during later stages of loading in all tests due to the effect of the lower lateral reaction on the outer face. The outer-face cracking pattern

seems to indicate that the disturbed end region extends for a distance equal to approximately 1.5 times the height of a spandrel. The area on the outer web face between the disturbed end region and the midspan flexural region also exhibited significant vertical flexural cracking. However, in most beams, inclined shear cracks were also observed in this region on the outer face. Note that the diagonal cracks in the end region are oriented orthogonally with respect



**Figure 8.** Inner-face cracking pattern for a representative corbelled spandrel (digitally enhanced cracks).





**Figure 9.** Outer-face cracking pattern for a representative spandrel with aspect ratio 7.5. Note: The midspan is near the right edge of photo.

to the shear and torsion cracks on the inside face. These cracks indicate that at high overloads, the plate bending stresses due to torsion exceed the diagonal compressive stresses due to shear. The three regions suggested by the cracking pattern are further defined and discussed in the companion paper.<sup>8</sup>

## Failure modes

Seven of the sixteen slender spandrels tested failed at their end regions along a skewed diagonal crack plane extending upward from the support. These seven spandrels were reinforced with excess flexural steel and were designed to prevent possible localized failure modes. End-region failures were observed in L-shaped spandrels and corbelled spandrels and in beams having aspect ratios of 7.5 and 4.6 (**Fig. 10**).

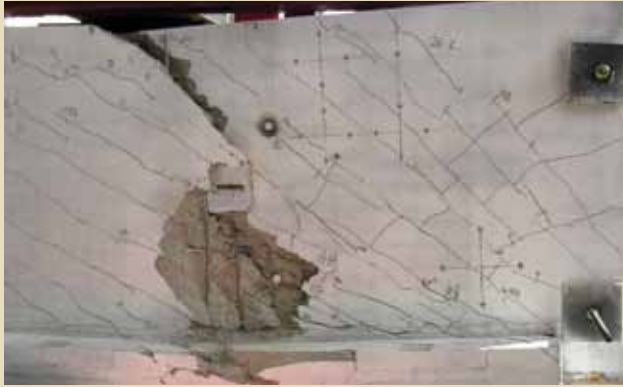
End-region failure modes were only observed in beams specially designed to force failures in the end region. These beams were particularly important to the research effort because they demonstrate the mechanism by which the end region of a slender spandrel beam could fail when overloaded in combined shear, flexure, and torsion, even if such failures only occurred at extreme overload in specially

configured test specimens. The observed end-region failure mode forms the basis of the rational design approach introduced in the companion paper.<sup>8</sup>

The typical end-region failure mode is shown in more detail in **Fig. 11** and **12**. The primary diagonal crack initiates at the face of the support and extends upward at an angle of approximately 45 deg. The crack crosses over the top of the web surface at a skewed angle of about 45 deg (**Fig. 11**). Finally, the crack returns along the same 45 deg angle to the face of the support on the outer face (**Fig. 12**). A key feature of the skewed end-region failure mode is the significant displacement of the failure surface out of plane. The failure suggests that the top lateral reaction causes the top corner of the web to bend outward, opening the diagonal crack. Simultaneously, the top edge of the web tends to twist out of plane at failure.

## Effect of parameters

The effects of selected key parameters on spandrel behavior are described in the next sections. A detailed description of the influence of parameters on behavior is presented elsewhere<sup>5</sup> for all parameters listed in Table 1.



SP3.8L60.45.P.O.E. (196 kip [872 kN])



SP4.8L60.45.P.O.E. (200 kip [890 kN])



SP10.8L60.45.R.O.E. (208 kip [925 kN])



SP12.8L60.45.P.O.E. (185 kip [823 kN])



SP17.8CB60.45.P.O.E. (200 kip [890 kN])



SP18.8CB60.45.P.S.E. (220 kip [979 kN])



SP20.10L46.45.P.O.E. (171 kip [761 kN])

**Figure 10.** End-region failure modes in beams with extra local and flexural reinforcement. Note: Each beam's main vertical reaction at failure is shown in parentheses.



**Figure 11.** Typical diagonal crack plane crosses the top of web at a skew.

## Open versus closed reinforcement

The most significant parameter examined by the research is the use of open web reinforcement compared with traditional closed stirrups. Three pairs of test specimens were included in the test matrix to highlight the differences between open and closed web reinforcement (**Fig. 13**). SP11 and SP13 were designed for torsion following current practice. Thus, the quantity of longitudinal and closed transverse reinforcement provided in these two beams was significantly more than that provided in companion beams with open reinforcement.

In general, service-level behavior was virtually identical when specimens with open web reinforcement are compared with those with closed reinforcement. The shear and torsion strength of end regions with closed reinforcement (designed using the procedure in the *PCI Design Handbook*)<sup>7</sup> is greater than the strength of end regions designed with open reinforcement according to the procedure proposed in the companion paper. However, the strengths of all end regions reinforced with open or closed stirrups were significantly higher than the factored design loads and were sufficient to ensure that failure modes outside the end region would always control. The factored design load ( $1.2DL + 1.6LL + 0.5SL$ ) was 126.6 kip (563.1 kN) for all six of the beams in Fig. 13. End-region failures occurred only when a given beam was specially reinforced to prevent other potentially controlling failure modes from occurring.

Measured deflection data demonstrate the similar behavior of beams with open and closed reinforcement. The measured load-deflection data at midspan are plotted in **Fig. 14** for SP12 (open reinforcement) and SP13 (closed reinforcement). Plots of the load versus vertical deflection were nearly identical for both beams through the factored load level. Both behaviors were linear to the service load.

The plotted experimental data show that the series of loading and unloading cycles is evident and that the residual deflection at zero applied load increases after each cycle. The horizontal segments in the load-deflection curves represent the effects of creep, where a beam continued to deflect slightly under constant applied load. The effects of creep are evident where the load was held for short observation periods during testing but are most notable during the 24 hr sustained loading at the factored load level.

The measured vertical end reaction is the entire reaction supported by a given beam, including the self-weight. Thus, plots of end reaction data do not start from the origin. The offset of approximately 22 kip (98 kN) represents the self-weight end reaction of the spandrel beam plus the short double-tee decks and loading system.

In this research, lateral deflections are highly significant due to the eccentrically applied loads. Lateral deflections were recorded for each spandrel at several locations,





**Figure 12.** View of typical diagonal crack plane on the outer web face.

including the top and bottom edges of the web at midspan. **Figure 15** shows measured lateral deflection data at these locations for SP12 and SP13 to further compare the effects of open reinforcement on behavior.






As with measured vertical deflections, the measured lateral deflections did not indicate any substantial difference in behavior due to open reinforcement through the factored load. At high levels of overload, the out-of-plane stiffness of SP13 (closed) was greater than that of SP12 (open), and the failure load was higher. SP13 (closed) contained 37% more web steel than SP12 (open).

The lateral deflection data plotted in Fig. 15 is typical for all spandrels with an aspect ratio of 7.5; that is, with increasing applied load, the upper edge of the web tended to move inward toward the double-tee decks at midspan, while the bottom edge of the web tended to move outward.

**Figure 16** compares the measured rotation of the web at midspan for the same two spandrels. Both spandrels exhibited the same type of out-of-plane behavior, and there was virtually no difference in measured rotations under service load. At higher loads, the beam with closed stirrups (SP13) had a higher rotational stiffness, but through the factored load level differences in measured rotations were minimal.

The performance advantage of closed stirrups compared with open reinforcement appears less significant when corbelled spandrel specimen SP17, reinforced with open web steel, is compared with corbelled spandrel specimen SP18, reinforced with special hooked stirrups. SP18 was an exact copy of SP17 except that all vertical web steel on the inner face was hooked over the top and bottom web (Fig. 2). Hooked web steel is not practical from the standpoint of production, but it is relevant for research purposes.

Comparison of SP17 and SP18 is useful because these two

	Open web reinforcement	Closed web reinforcement
Reinforced concrete L-spandrels	 <p>SP10.8L60.45.R.O.E. (208 kip [925 kN])</p>	 <p>SP11.8L60.45.R.C.E. (251 kip [1120 kN])</p>
Prestressed concrete L-spandrels	 <p>SP12.8L60.45.P.O.E. (185 kip [823 kN])</p>	 <p>SP13.8L60.45.P.C.E. (240 kip [1070 kN])</p>
Prestressed concrete corbelled spandrels	 <p>SP17.8CB60.45.P.O.E. (200 kip [890 kN])</p>	 <p>SP18.8CB60.45.P.S.E. (220 kip [979 kN])</p>

**Figure 13.** Matrix of failure modes for beams with open versus closed reinforcing schemes. Note: Failure loads are shown in parentheses for each beam.

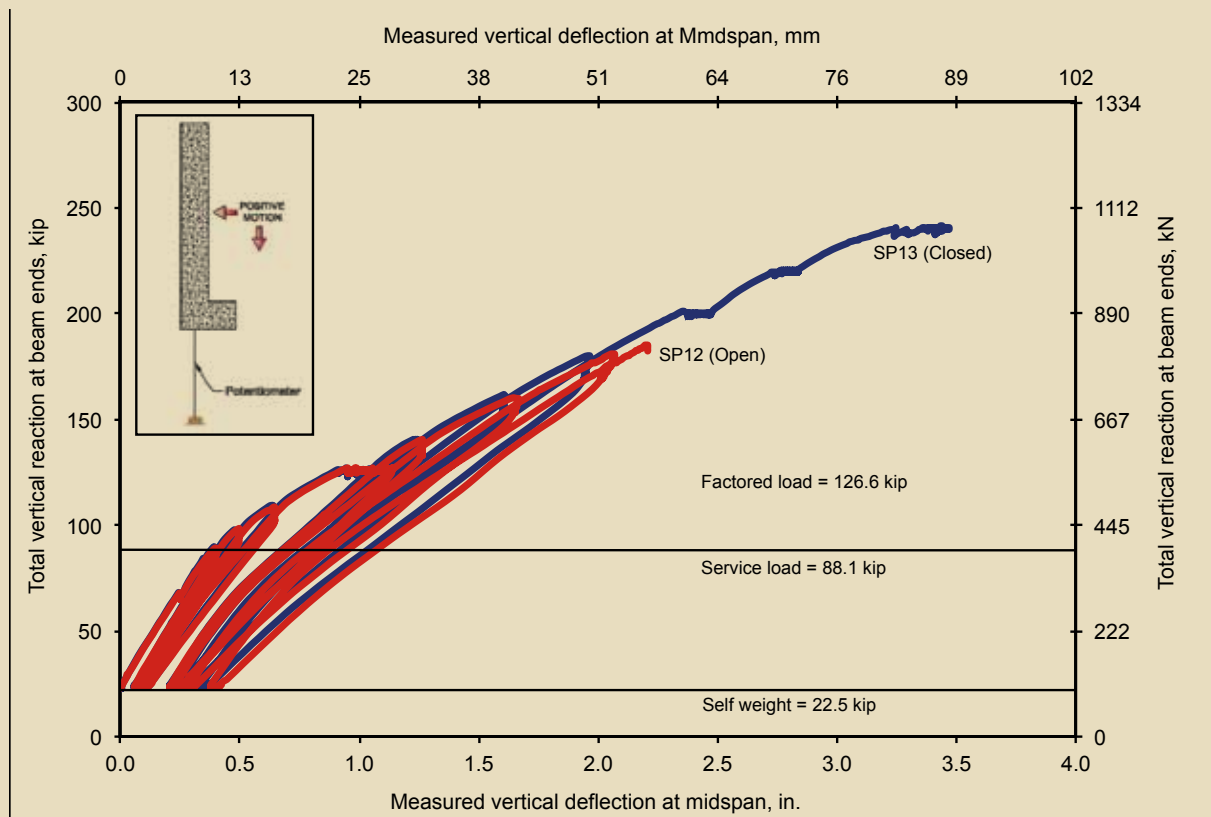


**Figure 14.** Measured load-vertical deflection response of two selected spandrels. Note: 1 kip = 4.448 kN.

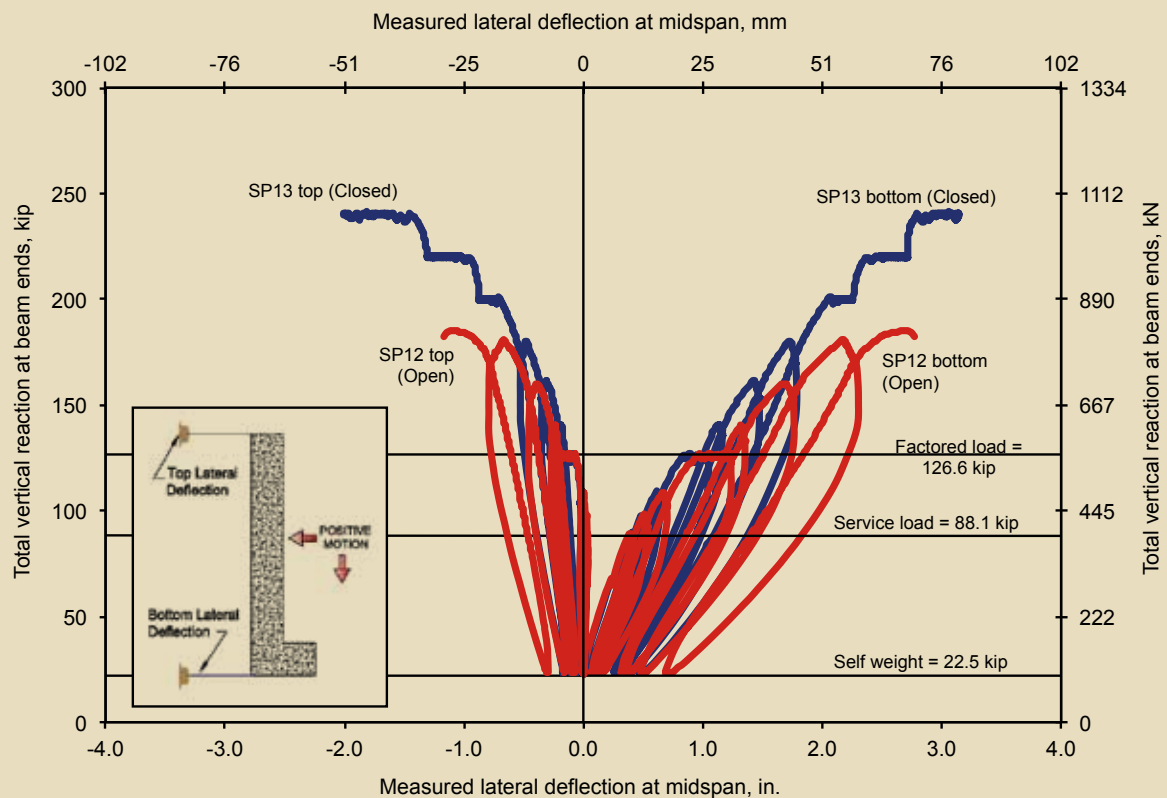


**Figure 15.** Measured lateral deflections at midspan for beams SP12 and SP13. Note: 1 kip = 4.448 kN.

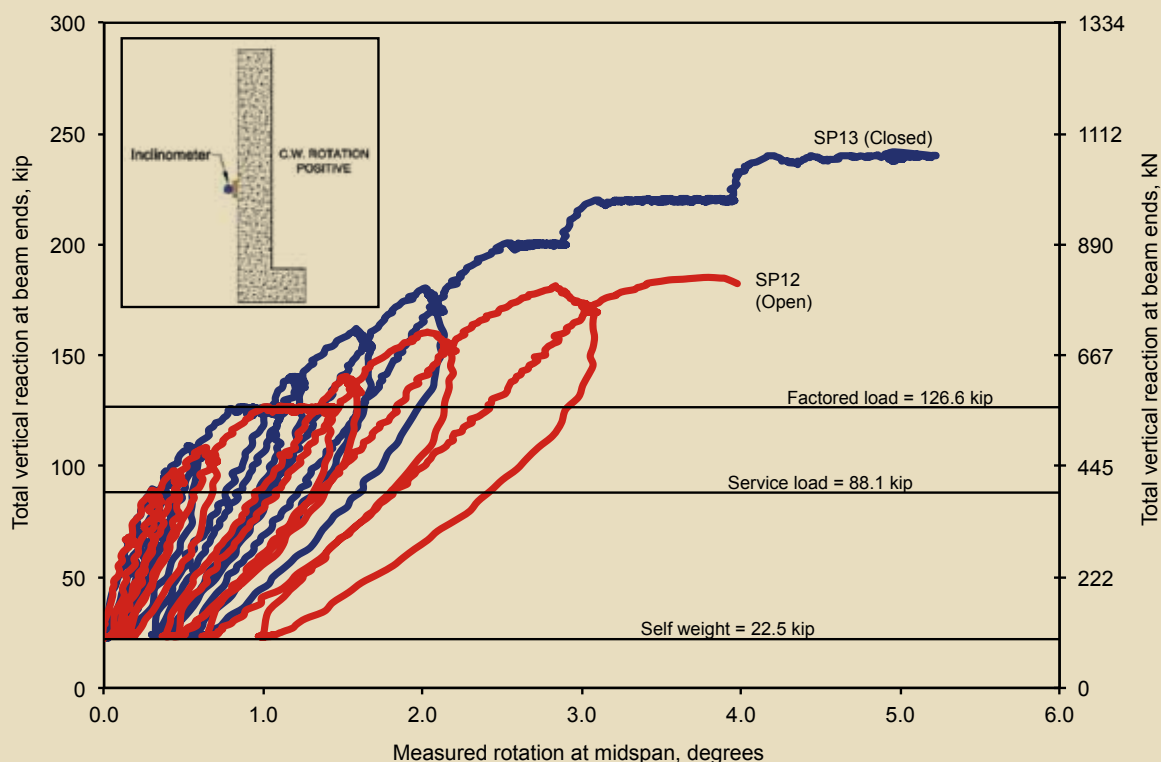


**Figure 16.** Rotation of web for spandrels SP12 and SP13. Note: 1 kip = 4.448 kN.

beams had the same quantities of vertical and longitudinal steel. Thus, any difference in performance is directly attributable to the steel crossing the top and bottom web faces. In other comparisons between open and closed reinforcement (SP10 versus SP11 and SP12 versus SP13), the beam with closed reinforcement was designed and detailed according to current practice. Thus, the beam with closed reinforcement had significantly more vertical and longitudinal web reinforcement (nearly twice the amount), in addition to having reinforcement in the form of closed ties.

The failure mode for SP17 was identical to that of SP18 (Fig. 17 and 18). Both beams failed along a skewed diagonal crack plane in their end regions. The vertical load-deflection behaviors at midspan (Fig. 19) were virtually identical to the load level of 200 kip (890 kN). The ultimate load of SP18 (special closed) was about 10% greater than the ultimate load of SP17 (open), suggesting that the steel on the top and bottom of the web face likely contributed to torsional resistance in the slender spandrel.

### Continuous ledges versus corbels

It was important for the research to examine both L-shaped spandrels and corbelled spandrels because both types of beams are commonly used by the industry. Test results indicate that the end-region failure mode takes the form of a skewed diagonal crack in both L-shaped spandrels and corbelled spandrels. SP12 and SP17 were both reinforced

with excess flexural and local reinforcement to allow the end-region behavior to be examined.

A general comparison between L-shaped spandrel deflection data and comparable corbelled spandrel deflection data indicates little difference in vertical load-deformation response for similarly reinforced beams. However, the outward lateral deflection at the bottom of the L-shaped spandrel is somewhat greater than that of the corbelled spandrel because the principal axes of the L-shaped spandrel are inclined. The effects of inclined axes and the differences between L-shaped spandrels and corbelled spandrels have been discussed elsewhere.<sup>5,10</sup>

### Typical beams without extra and special reinforcements

End-region failure modes were observed only in specimens designed with extra flexural steel and special ledge or hanger reinforcements. All beams reinforced at typical levels, as specified by ACI 318-08,<sup>6</sup> failed outside their end regions. Figure 20 presents a direct comparison between the failure modes of enhanced and typical specimens for three pairs of specimens. The observed failure modes for specimens designed with typical levels of reinforcement included localized ledge or corbel failures and flexural failure at midspan.

The only difference between the typical beam and the





**Figure 17.** Inner-face view of SP17 and SP18 after testing. Note: SP17 has open reinforcement, and SP18 has special closed reinforcement.

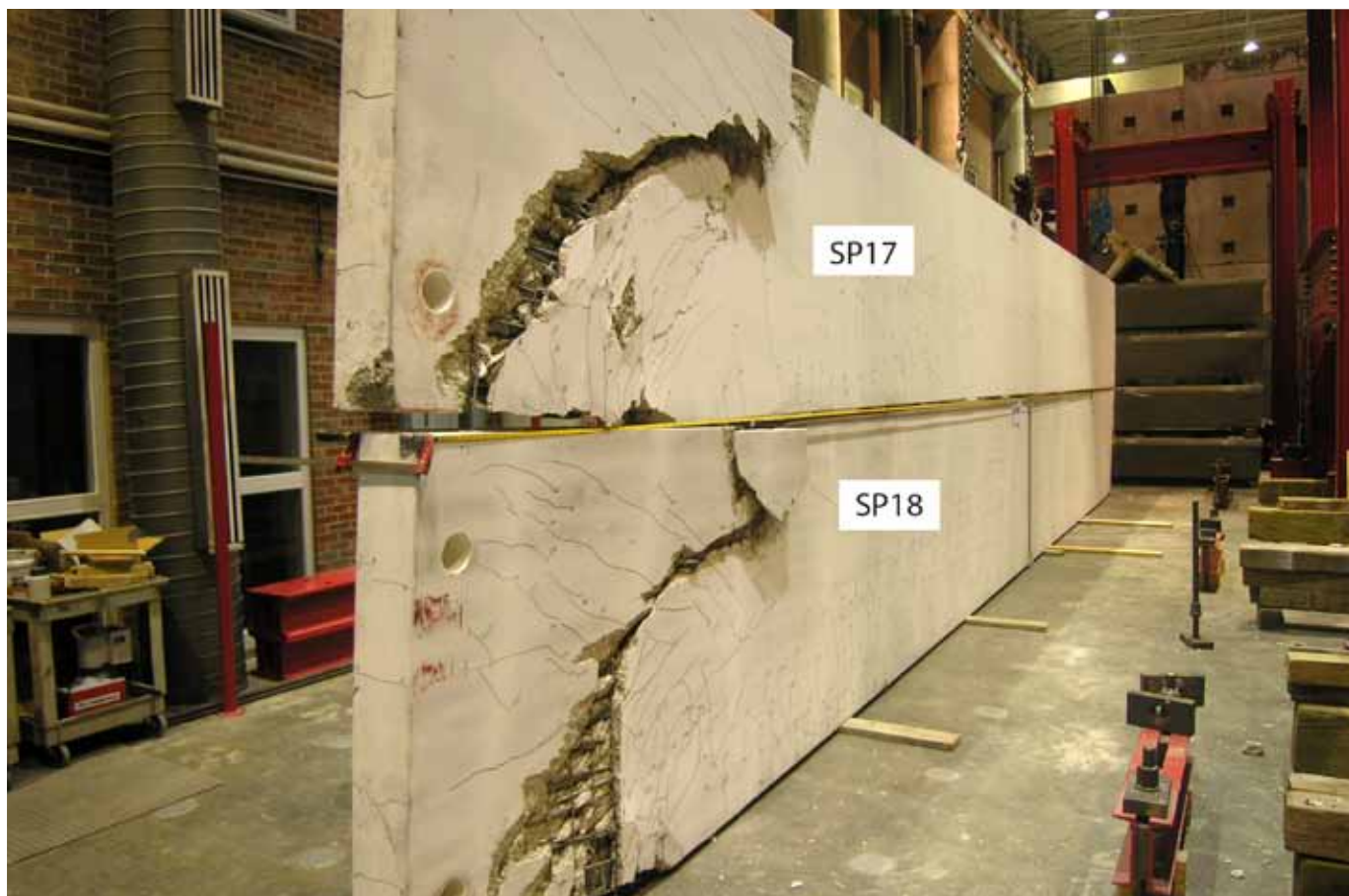
enhanced beam in each pair of specimens was that the enhanced beam had added partial-length mild steel and welded ledge reinforcements. The web reinforcement was identical for beams in a given pair.

**Figure 21** compares the vertical load-deflection behaviors of L-shaped spandrels SP12 (enhanced) and SP14 (typical), and **Fig. 22** compares the lateral-load-deflection behaviors. The flexural stiffness of SP14 (typical beam) is less than that of SP12 (enhanced beam), as would be expected. However, the lateral deflections measured at midspan for SP12 and SP14 are nearly identical, indicating that the excess flexural steel and local reinforcements did not alter behavior in the end region. The extra partial-length mild steel provided in the enhanced beams was held short of the end regions to avoid unintentionally improving end-region performance.

## Conclusion

The experimental program presented in this paper is one component of a larger research effort sponsored by PCI. The research effort also included significant finite-element and rational analysis and resulted in the development of a proposed rational design procedure. The companion paper presents the analytical work and design procedure. Tests conducted on 16 full-scale beams revealed that the end-region failures of slender precast concrete spandrel beams develop because of combined shear and torsion in the end region. The tests showed that spiral cracking and face-shell spalling did not develop. Rather, slender spandrel beams develop a tied-arch cracking pattern and if other failure modes are intentionally precluded, will ultimately fail along a skewed diagonal crack extending upward from the support.

Several conclusions are drawn based on the results of the experimental program. These conclusions apply to slender





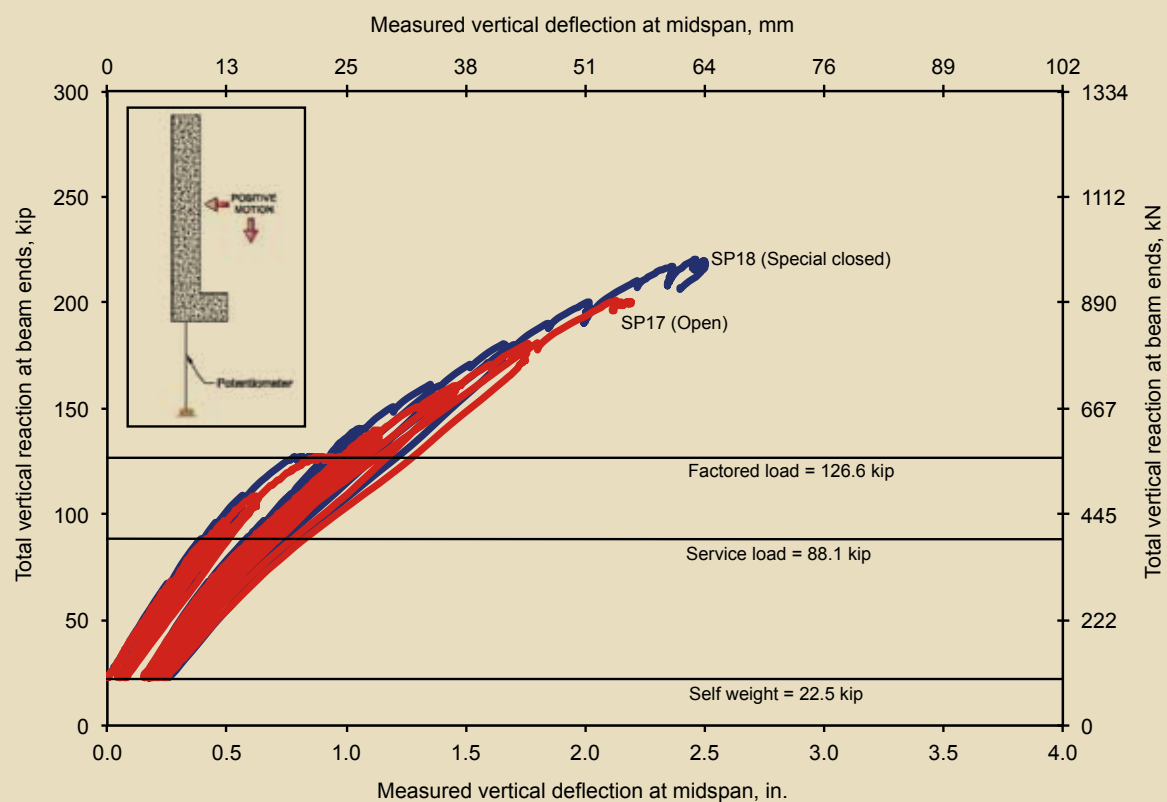



**Figure 18.** Outer-face view of SP17 and SP18 after testing. Note: SP17 has open reinforcement, and SP18 has special closed reinforcement.



**Figure 19.** Measured vertical deflections at midspan for SP17 (open) and SP18 (special closed). Note: 1 kip = 4.448 kN.



	Enhanced flexural and local reinforcement	Typical flexural and local reinforcement
Prestressed L-spandrels	 <p>SP12.8L60.45.P.O.E.</p>	 <p>SP14.8L60.45.P.O.T.</p>
Corbelled spandrels	 <p>SP17.8CB60.45.P.O.E.</p>	 <p>SP14.8L60.45.P.O.T.</p>
Prestressed L-spandrels aspect ratio 4.6	 <p>SP20.10L46.45.P.O.E.</p>	 <p>SP21.10L60.45.P.O.T.</p>

**Figure 20.** Comparisons of failure modes for enhanced versus typical reinforcement detailing.

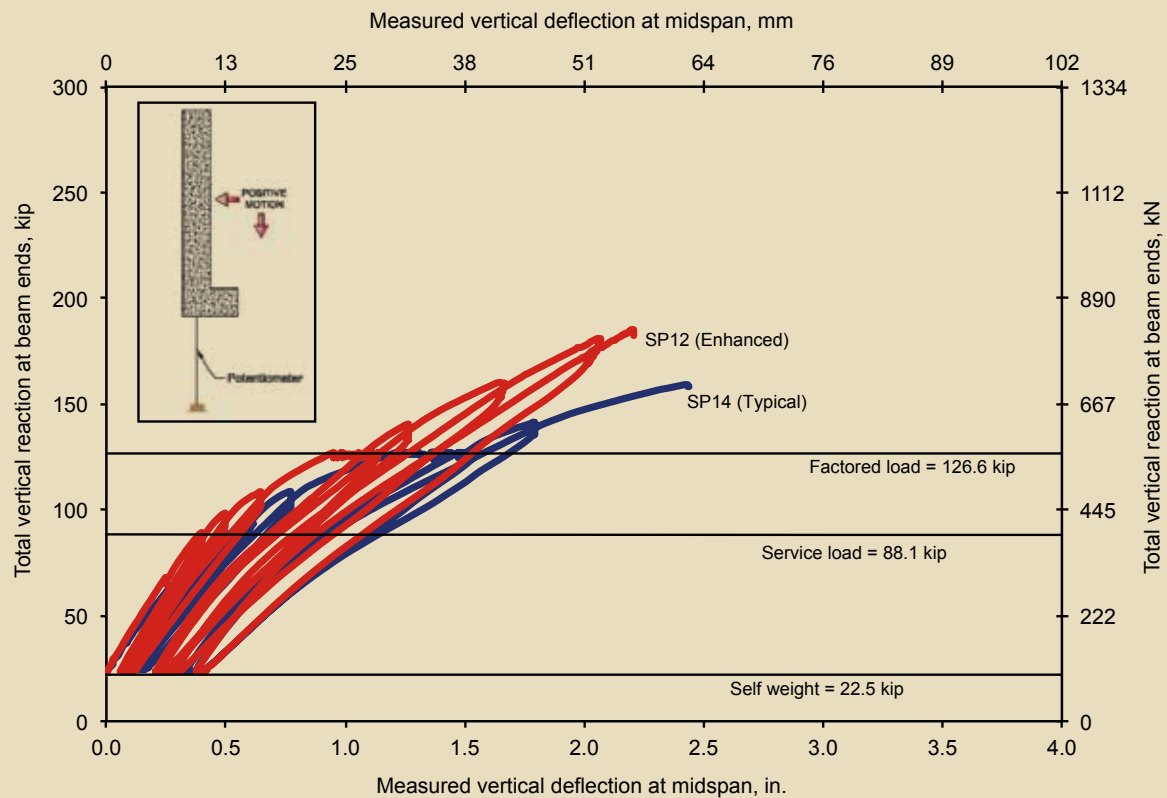


**Figure 21.** Measured vertical deflections from SP12 (enhanced) and SP14 (typical). Note: 1 kip = 4.448 kN.

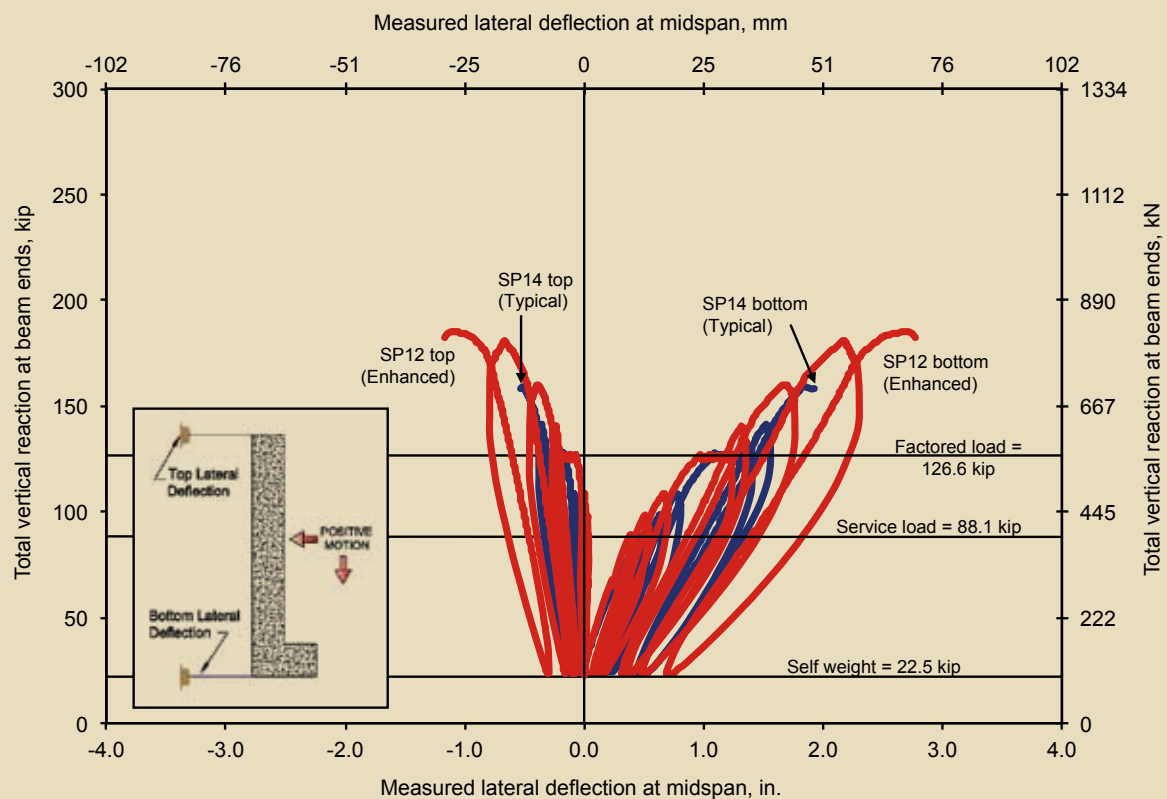


**Figure 22.** Measured lateral deflections from SP12 (enhanced) and SP14 (typical). Note: 1 kip = 4.448 kN.

spandrel beams that are simply supported with the web restrained laterally at each end. Such beams should have a distributed series of loads applied eccentrically along the bottom portion of the web through either a continuous ledge or corbels.

- Distinct differences in the cracking patterns of slender spandrel beams occur in three regions: the end region, the transition region, and the flexure region at mid-span.
- The shear and torsion resistance of tested slender spandrel beams with traditional closed stirrups was almost twice the factored load demand when reinforcement was proportioned according to the practice outlined in the *PCI Design Handbook*.
- The shear and torsion resistance of tested slender spandrel beams with open web reinforcement exceeded the factored load demand by 35% to 74% when reinforcement was proportioned according to the procedure described in the companion paper.
- The additional end-region strength provided by traditional closed stirrups compared with open web reinforcement is evident only when beams are subjected to extreme overload conditions by intentionally overreinforcing against other failure modes such as flexure or ledge failures.
- Open web reinforcement can provide virtually the same performance as traditional closed web reinforcement under factored design loads when slender spandrel beams are designed with typical levels of flexural and hanger reinforcement.
- The ledge and corbel failures observed in the typical specimens demonstrate that failure modes outside the end region will control the strength of properly detailed slender spandrel beams, regardless of whether open or closed web reinforcement is used.
- Several ledge punching failures occurred at loads below those predicted by the *PCI Design Handbook*.<sup>7</sup> Other researchers have observed similar results.<sup>11</sup> The interaction between ledge punching behavior and global flexure and shear appears to significantly reduce punching shear capacity. Although beyond the scope of this investigation, further study of ledge punching capacity is strongly recommended.

## Acknowledgments

This research was sponsored by the PCI Research and Development Committee. The work was overseen by an L-spandrel advisory group chaired by Donald Logan. The authors are extremely grateful for the support and guid-

ance provided by this group throughout all phases of the research. In addition, the authors would like to thank the numerous PCI producer members who donated test specimens, materials, and expertise in support of the experimental program.

## References

1. Hsu, Thomas T. C. 1984. *Torsion of Reinforced Concrete*. New York, NY: Van Nostrand Reinhold Publishers.
2. Mitchell, D., and M. Collins. 1976. Detailing for Torsion. *ACI Journal*, V. 73, No. 9 (September): pp. 506–511.
3. Collins, M., and D. Mitchell. 1980. Shear and Torsion Design of Prestressed and Non-Prestressed Concrete Beams. *PCI Journal*, V. 25, No. 4 (September–October): pp. 32–100.
4. Zia, P., and T. Hsu. 2004. Design for Torsion and Shear in Prestressed Concrete Flexural Members. *PCI Journal*, V. 49, No. 3 (May–June): pp. 34–42. was previously presented at the American Society of Civil Engineers Convention, October 16–20, 1978, Chicago, IL. Reprint #3424.)
5. Lucier, G., C. Walter, S. Rizkalla, P. Zia, and G. Klein. 2010. Development of a Rational Design Methodology for Precast Slender Spandrel Beams. Technical report no. IS-09-10. Constructed Facilities Laboratory, North Carolina State University, Raleigh, NC.
6. American Concrete Institute (ACI) Committee 318. 2008. *Building Requirements for Structural Concrete (ACI 318-08) and Commentary (ACI 318R-08)*. Farmington Hills, MI: ACI.
7. PCI Industry Handbook Committee. 2004. *PCI Design Handbook: Precast and Prestressed Concrete*. MNL-120. 6th ed. Chicago, IL: PCI.
8. Lucier, G., C. Walter, S. Rizkalla, P. Zia, and G. Klein. Development of a Rational Design Methodology for Precast Concrete Slender Spandrel Beams: Part 2, Analysis and Design Guidelines. *PCI Journal*, forthcoming.
9. American Society of Civil Engineers (ASCE). 2010. *Minimum Design Loads for Buildings and Other Structures (7-10)*. Reston, VA: ASCE.
10. Logan, D. 2007. L-Spandrels: Can Torsional Distress Be Induced by Eccentric Vertical Loading? *PCI Journal*, V. 52, No. 2 (March–April): pp. 46–61.

11. Klein, Gary J. 1986. *Design of Spandrel Beams*. PCI specially funded research and development program research project no. 5 (PCISFRAD #5). Chicago, IL: PCI.
12. Raths, Charles H. 1984. Spandrel Beam Behavior and Design. *PCI Journal*, V. 29, No. 2 (March–April): pp. 62–131.
13. Lucier, G., S. Rizkalla, P. Zia, and G. Klein. 2007. L-Shaped Spandrels Revisited: Full-Scale Tests. *PCI Journal*, V. 52, No. 2 (March–April): pp. 62–76.

## Notation

$b$  = web thickness

DL = dead load

$h$  = beam height

LL = live load

SL = snow load

## About the authors



Gregory Lucier is a laboratory manager for North Carolina State University in Raleigh, N.C.



Catrina Walter is an engineer for BergerABAM in Federal Way, Wash.



Sami Rizkalla is a Distinguished Professor at North Carolina State University.



Paul Zia is a Distinguished University Professor Emeritus at North Carolina State University.



Gary Klein is an executive vice president and senior principal for Wiss, Janney, Elstner Associates Inc. in Northbrook, Ill.

## Synopsis

This paper summarizes test results of an extensive experimental program undertaken to develop a rational design procedure for precast concrete slender spandrel beams. Experimental research findings presented in this paper are used to propose a rational design procedure that will be presented in a forthcoming com-

panion paper. The research introduced significantly simplified detailing requirements for the end regions of precast concrete slender spandrel beams. Such regions are often congested with heavy reinforcing cages when designed according to current procedures.

In total, 16 full-scale precast concrete spandrel beams were tested to failure to study the limit state behavior. Each specimen was loaded through full-scale double-tee deck sections to mimic typical field conditions. Three of the specimens were designed and detailed with closed stirrups, according to current practice, and served as controls for the experimental program. The remaining thirteen specimens were designed with various configurations of open web reinforcement. Several specimens were specially configured with flexural, ledge/corbel, and hanger reinforcement in excess of what would be provided in a normal design. The enhanced reinforcement helped to delay typical midspan and local failure modes and allowed for observation and study of failure modes in the end region.

The experimental results, combined with the analytical results and rational modeling in the companion paper, demonstrate that properly designed open web reinforcement is a safe, effective, and efficient alternative to traditional closed stirrups for precast concrete slender spandrel beams that have an aspect ratio of 4.6 or greater.

## Keywords

Beam, failure, load, reinforcement, spandrel, torsion.

## Review policy

This paper was reviewed in accordance with the Precast/Prestressed Concrete Institute's peer-review process.

## Reader comments

Please address any reader comments to [journal@pci.org](mailto:journal@pci.org) or Precast/Prestressed Concrete Institute, c/o *PCI Journal*, 200 W. Adams St., Suite 2100, Chicago, IL 60606. 